Unmanned Logistics Vehicle Control based on Path Tracking Control Algorithm

Menglin Wu*, Zhenyu Liu
Department of Economic Management, Zhengzhou Vocational College of Finance and Taxation, Zhengzhou 450000, China
E-mail: 17335743056@163.com
*Corresponding author

Keywords: unmanned logistics vehicles, path tracking control algorithms, model predictive control algorithms, logistics industry, variable structure control

Received: March 20, 2024

The logistics industry has made significant progress in recent years. However, there are still issues with low operational efficiency and high costs. Unmanned logistics vehicles have gained attention as an efficient and intelligent mode of transportation with the rapid development of the industry. The study utilizes an advanced path tracking control algorithm, in combination with model predictive control technology, to monitor and adjust the path, speed, and direction of unmanned logistics vehicles in real-time. The aim is to enhance the stability, safety, and efficiency of travel. The experiments revealed that the average accuracy of path deviation prediction of the proposed model on two different datasets is 88.33% and 82.1%, which is 3.96% and 4.72% higher than that of the control model, respectively. The control accuracy of the proposed model reached 94.19% on the KITTI Vision Benchmark Suite dataset and 95.61% on the CARLA Simulator dataset, which are both higher than the other control models. In addition, the study also tested the proposed model for energy consumption, controller switching frequency, lateral error and other indexes, and the findings revealed that the proposed model of the study exhibits high stability and efficiency. This research not only provides new ideas for the control of unmanned logistics vehicles, but also verifies the effectiveness of the control strategy through experiments.

Povzetek: Študija vpelje napredni algoritem za sledenje poti v kombinaciji s prediktivnim modelom za nadzor brezpilotnih logističnih vozil, kar izboljšuje stabilnost, varnost in učinkovitost prevoza z visoko kvaliteto nadzora.

1 Introduction

In traditional logistics transportation, manual operation and scheduling are essential, but manual operation and scheduling have defects such as high labor cost, inefficient operation, prone to human error, and lack of real-time monitoring and data analysis [1-2]. With the rapid development of electronic, communication and computer technologies, unmanned logistics vehicles (ULV) control has become an important way to solve the efficiency and safety problems in the logistics industry [3]. Compared to traditional logistics, ULVs have improved in path tracking, speed control and safety, which improves logistics efficiency and reduces operational costs. ULV control refers to the use of path tracking control (PTC) technology and driverless technology to realize autonomous operation and control of logistics vehicles [4]. By introducing driverless technology and ULV algorithms, the transportation efficiency of logistics vehicles can be improved, the risk of accidents can be reduced, and the pressure on human resources can be alleviated. In addition, research on ULV algorithms has benefited from advances in computer vision, sensor technology and artificial intelligence [5]. With the help of high-precision maps, LIDAR, cameras, and other sensors, ULVs can sense and understand their surroundings in real time to better plan their paths and avoid obstacles. There are two innovations in this research: first, the linear six-degree-of-freedom (L6DOF) vehicle dynamics model (V-MPC) is optimized based on variable structure control (VSC) to simplify the output structure of the dynamics model. The second point is that the objective function and output function of the model are optimized using model predictive control (MPC), which improves the stability of the model path tracking. The structure of this article is divided into six parts: The first part is related work, which will review the literature to summarize the development status, application scenarios, etc. of ULV technology. The second part is the methodology, which constructs the unmanned vehicle operation model through MPC and VSC algorithms. The performance test, which is the third section, is how this experiment verifies the suggested model's functionality. The fourth part is the discussion, which compares the design method with relevant literature and analyzes its

advantages. The study's weaknesses and findings are compiled in the conclusion, which makes up the fifth section. The sixth part is Ethical and Safety Considerations, which introduces the ethical and safety standards followed by the design method.

ULV is the current hotspot in the research of driverless technology, and many researchers have explored for the realization method of ULV. Hang et al. proposed a novel four-wheel steering electric vehicle as an automatic ground vehicle. To realize the automatic driving of this automatic ground vehicle, they constructed a linear variable parameter system model to adapt the ULV apparatus to different longitudinal speeds and road friction coefficients. The experimental results indicated that the linear variable-parameter system model constructed by the study exhibited better path tracking performance [6]. Path tracking is one of the main responsibilities of self-driving automobiles, as discovered by Chen et al. They consequently used deep neural network techniques to optimize path tracking. In this study, a combination of proximal policy optimization and pure optimization was chosen to build the vehicle controller architecture. The combination of the two algorithms makes the overall operation of the control system more robust and improves the additivity of the controller. The results indicated that the optimized control system's path tracking capability was significantly enhanced under low-speed driving conditions [7]. Lin et al. used the ULV algorithm to optimize a linear three-degree-of-freedom V-MPC and proposed an integrated control method combining the MPC and ULV algorithms. The MPC was typically used to avoid yaw, while the ULV algorithm maintains vehicle roll stability by controlling the braking force of each tire. The study's comparison of the suggested model with popular models like CarSim revealed that the enhanced control system, which uses the ULV algorithm, produces smoother outcomes [8]. Sun et al. proposed a fast non-singular terminal sliding mode control strategy with a double hidden layer output feedback neural network. The strategy improved the sliding mode control using feedback neural network and ULV algorithm, and constructed vehicle kinematics and dynamics models. Simulation experiments yielded that the control algorithm of the proposed model has significant advantages such as high tracking accuracy, fast convergence, and robustness compared with the traditional sliding mode controller [9].

MPC is one of the commonly used algorithms in current dynamics research, and more extended applications of this algorithm have emerged. Pan et al. proposed a new multilayer graph architecture based on the MPC algorithm to achieve scalability of interaction networks. The architecture established formation control laws for autonomous formation, formation maintenance, collision and obstacle avoidance using the MPC algorithm on the basis of multilayer graphs. Finally, the experiments adopted the proposed framework to accomplish the formation maintenance and trajectory tracking tasks in the constraint space, which verified the feasibility of the proposed framework [10]. Çimen et al. combined the MPC algorithm with the firefly optimization algorithm, thus proposing a new optimization algorithm. The optimization algorithm was used to study single-peak, multi-peak, composite and CEC-C06 2019 benchmark optimization and optimal design parameter determination problems. It was experimentally verified that the proposed model possesses lower loss and higher performance efficiency than the current common models of the same type [11]. Beus et al. proposed a load/frequency controller for hydraulic turbine governor based on MPC. This controller was updated by linearly predicting the operating points of the model parameters, thus greatly improving the stability and operating efficiency of the frequency controller. The proposed controller was experimentally compared with several state-of-the-art controllers such as particle swarm optimization-based PI controller. Additionally, the findings showed that the research's suggested model benefits from having a straightforward structure and quick calculation [12]. A hierarchical non-linear MPC method for cooperative control of vehicle-vehicle networks was proposed by Liu et al. The algorithm employs a multilayer structure and solves its optimization problem by continuous/generalized minimum residual method. To enhance tracking performance, the algorithm also included a controller with a double-loop structure. According to experimental findings, the suggested method outperforms the most advanced vehicle cooperative control models in terms of stability and error rate, proving its usefulness in real-world scenarios [13].

To clarify the advantages and disadvantages of PTC technology and MPC technology, the research summarized the literature review in Table 1. Further optimization is needed based on current research due to the low computational efficiency and implementation difficulties found in previous studies.

Table 1: Summary of related work content

Reference	Improvement/Application direction	Results
[6]	This study was based on a linear variable parameter system model to modify four-wheel steering electric vehicles	The linear variable parameter system model has better path tracking performance
[7]	This study utilized deep neural network technology to optimize path tracking algorithms	Under low-speed driving conditions, the path tracking ability of the optimized control system is significantly improved
[8]	This study optimized the linear three degree of freedom V-MPC using the ULV algorithm	The enhanced control system using ULV algorithm produces smoother results
[9]	This study was based on optimizing the path tracking algorithm using a dual hidden layer output feedback neural network	The optimized control algorithm has the characteristics of high tracking accuracy and fast convergence speed
[10]	This study proposed a multi-layer graph architecture based on the MPC algorithm	This architecture diagram completes formation maintenance and trajectory tracking tasks in the constrained space
[11]	This study optimized the MPC algorithm based on fireflies	The optimized algorithm has lower loss and higher performance efficiency
[12]	This study proposed a load/frequency controller for a water turbine governor based on MPC	Proposed model has a simple structure and fast computing power
[13]	This study proposed a hierarchical nonlinear MPC method for vehicle network collaborative control	The effectiveness of this method in real-life scenarios has been verified through experiments

In summary, ULV has now achieved greater results in small unmanned vehicle applications after recent years of development. However, the current commonly used ULV algorithms still have defects such as high computational complexity and difficult to realize. Therefore, the research tries to use VSC algorithm and MPC algorithm to optimize the more complex L6DOF, aiming to construct a stable and efficient ULV control algorithm.

2 Improved control of unmanned logistics vehicles based on VSC and MPC algorithms

ULV has steadily come to dominate the logistics and transportation fields due to the industry's rapid development as well as the ongoing advancements in science and technology. The traditional manual driving logistics vehicles have some limitations in terms of efficiency, safety and environmental protection. To overcome these shortcomings, the study uses advanced control algorithms, such as MPC and vehicle stability control, to construct a stable and efficient ULV control model. This will help promote technological innovation and sustainable development in the logistics industry.

2.1 Path tracking model based on VSC

The VSC algorithm is a control strategy whose core idea is to utilize sliding modal hyperplanes to achieve fast, non-linear switching of the dynamic characteristics of the system [14-15]. This algorithm is robust in dealing with uncertainties and perturbations because the sliding modal hyperplane can be adaptively adjusted according to the changes in the system state. In ULV, the VSC algorithm is used to design controllers that enable the system to track the desired path quickly and accurately [16]. The VSC approach has garnered a lot of interest in the ULV sector because of its benefits, which include quick response times and insensitivity to changes an system parameters [17]. In order to better study the path selection condition of logistics vehicles on the way of transporting goods, it is necessary to construct a V-MPC. A L6DOF is used in this study. It is assumed that c denotes the spacing from the right wheel of the vehicle to the center of mass and d denotes the spacing from the left wheel to the center of mass. In order to facilitate the analysis in hand, the study establishes a new temporary coordinate system for each analysis point, and the temporary coordinate system is $x-y$. Then F_x denotes the force received in the direction of x of the temporary coordinate system, and F_y denotes the force received in the direction of y of the temporary coordinate system. The structure of the model is shown in Figure 1.

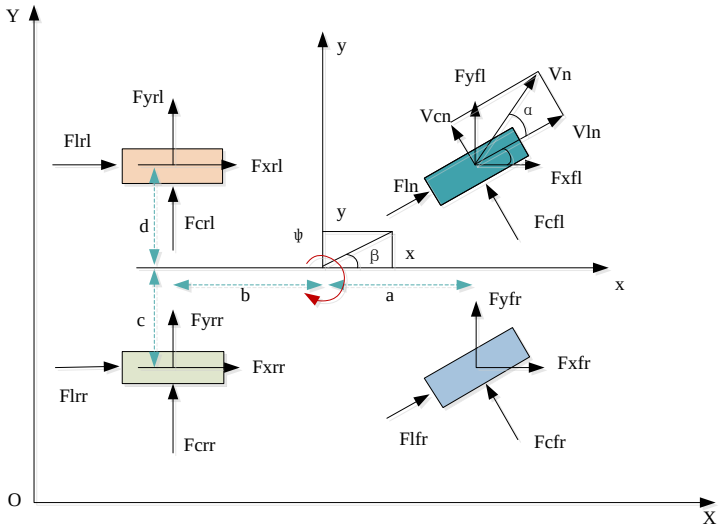

Figure 1: Hand analysis of linear six-degree-of-freedom vehicle dynamics model

F_c in Figure 1 shows the lateral force on the vehicle tires, which has a significant impact on the handling, stability and safety of the vehicle. F_l, on the other hand, denotes the longitudinal force, which acts similarly to the lateral force and are both forces that maintain stable vehicle motion. In addition, α, β is the center of mass and the lateral deflection angle of the tire in the figure, respectively, and δ denotes the tire deflection angle. If the vehicle's power wheel deflection angle stays constant, the vehicle's motion will likewise be constant according to this model [18]. Currently, equation (1) displays the relationship between the steering wheel rotation angle and the transverse angular velocity at the vehicle's center of mass. This ratio can reflect the stability of the current state of the vehicle.

$$G_\omega = \frac{v_x}{i_{sw} L\left(1+\alpha v_x^2\right)} \tag{1}$$

In equation (1), ω denotes the pendulum angular velocity at the center of mass, and L denotes the horizontal distance between the front and rear axles of the vehicle. v_x denotes the velocity of the horizontal motion of the vehicle, and i_{sw} denotes the ratio of the front wheel angle to the control angle. K denotes the stabilization factor, and G_ω denotes the ratio of the pendulum angular velocity at the center of mass to the steering wheel turning angle. The value of K is related to the mass of the vehicle, the distance between axles, etc., and its computational expression is shown in equation (2) in s^2/m^2.

$$K = \frac{m}{L^2}\left(\frac{b}{C_f} - \frac{a}{C_r}\right) \tag{2}$$

In equation (2), C_f denotes the front tire lateral deflection stiffness and m denotes the mass. b stands for the distance between the vehicle's front axle and center, while C_r stands for the rear tires' stiffness in terms of lateral deflection. The a represents the separation between the vehicle's center and rear axle. In addition, the vehicle center of mass lateral deflection (MLD) also has a large effect on vehicle stability, the center of MLD affects the stability of vehicle motion by increasing the steering wheel stability [19]. The gain coefficient of center of MLD on steering wheel stability is shown in equation (3).

$$G_\beta = \frac{b + \frac{mv^2 a}{LC_r}}{i_{sw} L\left(1+Kv_x^2\right)} \tag{3}$$

In equation (3), G_β denotes the gain coefficient of the center of MLD on steering wheel stability. β denotes the center of MLD angle. If the vehicle transverse swing angle and the horizontal direction of the running state remain unchanged, at this time the instantaneous speed of the vehicle doing circular motion can be approximated as the tangential direction of the speed. At this time, the instantaneous velocity and motion path of the vehicle are shown in Figure 2.

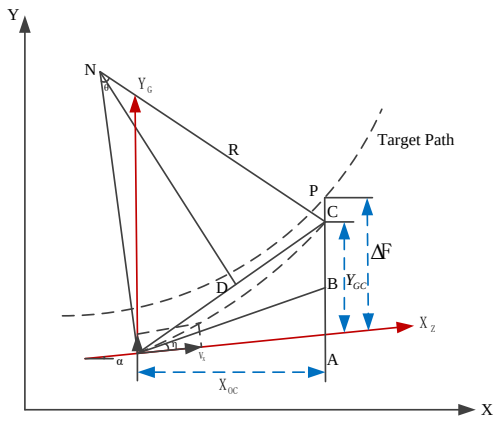

Figure 2: Instantaneous velocity and motion path diagram of the vehicle

In Figure 2, $\angle CGB$ denotes the chordal tangent angle of the vehicle's trajectory, and therefore $\angle CGB$ is equal to the $\frac{1}{2}$ of the circumferential angle of the vehicle's trajectory. Therefore, the position of the vehicle in the direction of Y_G changes as shown in equation (4).

$$y_G = \tan\left(\frac{\theta}{2}+\beta\right)x_G \tag{4}$$

In equation (4), y_G represents the displacement in the Y_G direction on the $X_G - Y_G$ A coordinate system established with the vehicle's last moment of motion point G as the origin, and x_G represents the displacement in the X_G direction. When the vehicle is in the process of uniform speed steering, the relationship between the angles in equation (4) can be deduced from the ideal state of the steering wheel angle of rotation angle of the expression, which becomes larger as shown in equation (5).

$$\delta_{sw} = \frac{2\arctan\left(\frac{\Delta f}{v_x t_p}\right)}{G_\omega t_P + 2G_\beta} \tag{5}$$

In equation (5), Δf denotes Y_{GC} in Figure 2 and t_p denotes the time period. The kinetic model also serves to predict the vehicle motion deviation. The algorithm's prediction of the deviation is related to the projected distance L_{ag} from the point of motion to the predicted point at the previous moment, and the expression for the calculation of the motion deviation is shown in equation (6).

$$\Delta f = \frac{d_{la}}{\cos\Delta\varphi} = \frac{d_{la}}{\cos\left(\arcsin\left(\frac{d_{la}}{L_{ag}}\right)\right)} \tag{6}$$

In equation (6), d_{la} denotes the spacing between the predicted path to the projection point. Δf denotes the motion deviation of the vehicle, and $\Delta\varphi$ denotes the angle between the target path and the actual path. At this point, the non-L6DOF V-MPC is constructed, so the study needs to optimize this model according to the VSC algorithm. Convergence law design is an important task in the design of VSC algorithm. Convergence law is a control strategy designed to make the system state gradually converge to the target state or desired value [20]. The role of convergence law design is to improve the stability, tracking performance and robustness of the system by gradually adjusting the control signals so that the system state gradually converges to the target state. The study uses the exponential convergence law to optimize the model, and the mathematical expression of the exponential convergence law is shown in equation (7).

$$s = -\eta\,\mathrm{sgn}(s) - ks \tag{7}$$

In equation (7), $\mathrm{sgn}(.)$ denotes the sign function, η, k both denote the parameters of the exponential convergence law, and both are rational numbers greater than zero. s denotes the convergence law value. In addition, vibration elimination is also a more important part. Vibration elimination requires the definition of the saturation function, and the expression of the conservation function is shown in equation (8).

$$sat(s) = \begin{cases} \mathrm{sgn}(s), |s| > \psi \\ s, |s| \le \psi \end{cases} \tag{8}$$

In equation (8), ψ denotes the width of the boundary layer. $|.|$ denotes the absolute value taken. In the dynamics model, the setting of the boundary layer can affect the stability and convergence of the simulation. Reasonable setting of the boundary layer can reduce the numerical error and oscillation phenomenon, improve the simulation effect.

2.2 Path tracking model construction based on MPC improvement

Based on the above, the study constructed a non-L6DOF path-tracking model based on VSC, but the switching process of VSC usually introduces a control pulse, i.e., a sudden change of the control input on the sliding mode surface [21]. This impulse signal may lead to a non-ideal response of the system, and therefore new methods need to be introduced to further optimize the model. The MPC algorithm is an optimization control method that is widely used in fields such as industrial process control and motor vehicle control. Utilizing a dynamic model of the system, it makes predictions and solves an optimization problem in each control cycle to determine the ideal control inputs. Its basic steps include system modeling, prediction, optimization problem definition, optimization solution and application of control inputs

[22]. The algorithm is able to take into account the non-linear characteristics and constraints of the system as well as dynamic optimization during each control cycle. The control schematic of the MPC algorithm is shown in Figure 3.

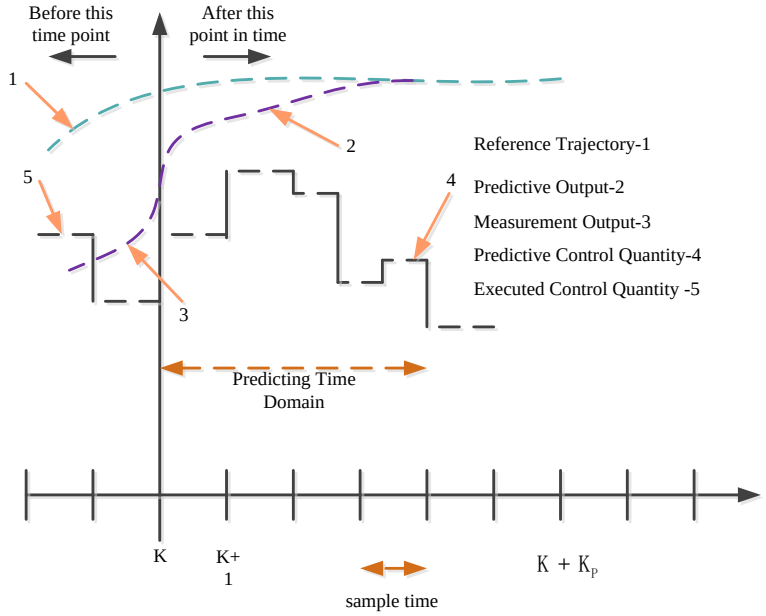

Figure 3: MPC algorithm control principal diagram

The MPC algorithm redefines the instantaneous states, control parameters, and outputs of the above V-MPC, which are shown in equation (9).

$$\begin{cases} \xi(t) = f\left(\xi(t), u(t)\right) \\ \zeta(t) = h\left(\xi(t), u(t)\right) \end{cases} \tag{9}$$

In equation (9), $\xi(t)$ is the state vector of the model and $\zeta(t)$ denotes the output of the model. t denotes the time and $u(t)$ denotes the control vector of the model. Discreteization of the dynamics model is also required when instantaneous states, control parameters, and outputs have been redefined. The original non-linear model is to be transformed into a discrete linear time-varying model using the discretization method. Equation (10) displays the state vector expression following the discretization process.

$$A\xi(t) = B\xi(t) + Cu(t) \tag{10}$$

In equation (10), A, B, C are all discretized process variables, and the specific value of A, B, C can be derived by solving equation (9) in a generalized way. Moreover, the discretized state vector of $t+1$ moment is calculated as shown in equation (11).

$$\xi(t+1) = B'\xi(t) + C'u(t) + d_t \tag{11}$$

In equation (11), B', C' is the discretized process variable and d_t is the special solution of equation (9) at moment t. The kinetic model can be iterated after discretization so as to calculate the discrete values at each moment. Objective function design, constraint design, and prediction function design are needed after the model is discretized. Among them, the objective function design plays a key role, and the reasonable selection and definition of the objective function can clarify the problem objective, guide the problem modeling, provide measures and constraints, and affect the behavior and final results of the optimization algorithm [23]. Assuming that N_p denotes the prediction step and Y_p denotes the output prediction value. Equation (12) displays the expression for the MPC algorithm's objective function.

$$J\left(\xi(t), \Delta U(t), \varepsilon\right) = \sum_{i=1}^{N_p} \| Y_p(k+i) - Y_{ref}(k+i) \|_Q^2 + \sum_{i=1}^{N_c} \| \Delta u(k+i) \|_R^2 + \rho\varepsilon^2 \tag{12}$$

In equation (12), N_c denotes the control step size and ε denotes the relaxation factor. $\|.\|$ denotes the Euclidean paradigm operation, Y_{ref} denotes the control output ideal, and Q, R, ρ denotes the corresponding weight matrix. Path tracking accuracy and stability can be increased by the system by tracking the intended path more precisely and by decreasing the goal function. In addition to guaranteeing that the state of the system is always within the safety range, the model constraints also ensure the viability of the control inputs and state variables [24]. The performance of the model and its ability to adapt to different demands can be effectively improved by setting constraints reasonably. The constraints of the model of this research are mainly for four aspects: output, control weight, weight change rate, and relaxation factor. The specific constraints are shown

in equation (13).

$$\begin{cases} Y_{\min} \le Y(t) \le Y_{\max} \\ u_{\min} \le u(t) \le u_{\max} \\ \Delta U_{\min} \le \Delta U \le \Delta U_{\max} \\ \varepsilon_{\min} \le \varepsilon \le \varepsilon_{\max} \end{cases} \tag{13}$$

In equation (13), $Y(t)$ denotes the vehicle output quantity and $u(t)$ denotes the core control quantity of the model. ΔU denotes the weight change of the control quantity and ε denotes the relaxation factor. The wrong iteration loop will end earlier after the model is given the constraints, so the computational efficiency of the model is further improved.

Currently, the model's output function differs from the pre-optimization, and equation (14) displays the optimized prediction function's expression.

$$y(t) = \varepsilon\xi(t) + \tau\Delta U(t) + \mu_t \tag{14}$$

In equation (14), μ_t denotes the amount of model control at the current moment, and the acquisition of the $\xi(t)$ value relies on the sensors of the simulation model. The introduction of the MPC algorithm allows the model to perform a comprehensive path deviation analysis and correct the route in a timely manner through multi-point prediction. The structure of multi-point deviation prediction is shown in Figure 4.

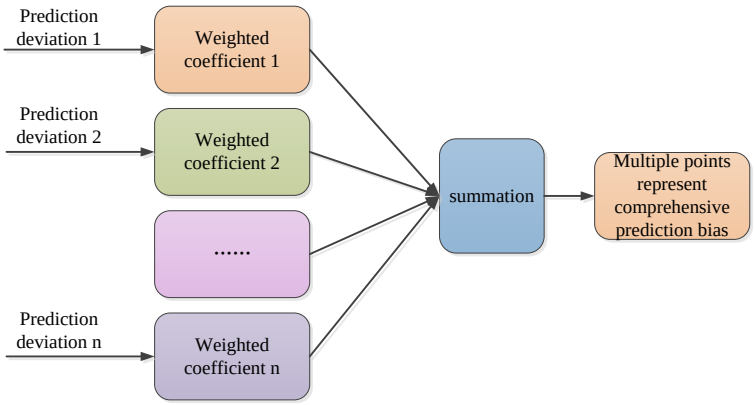

Figure 4: Structure diagram of multi-point deviation prediction

After the optimization of VSC algorithm and MPC algorithm, the V-MPC can be improved in terms of control performance, stability, tracking performance and energy consumption optimization. These optimizations can improve the vehicle handling, safety and energy efficiency performance. The flow chart of the optimized V-MPC operation is shown in Figure 5.

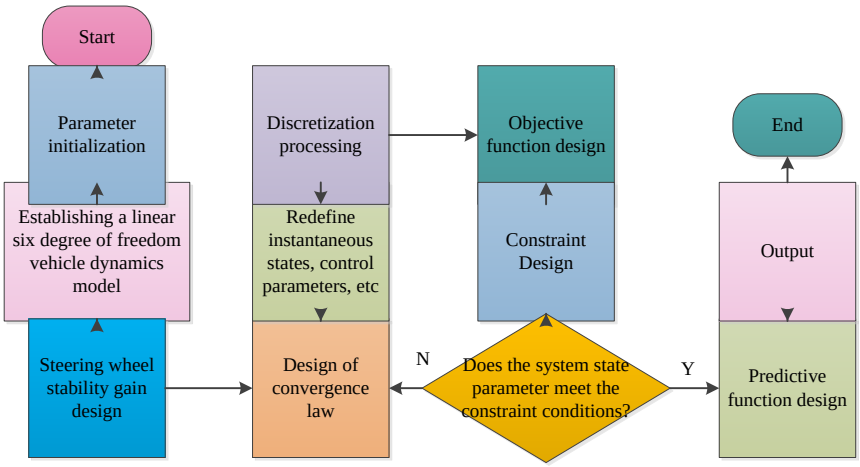

Figure 5: V-MPC model operation flow chart

In practical logistics scenarios, the proposed model addresses the issue of low accuracy in traditional PTC algorithms by enhancing the path tracking algorithm. This improvement concept also has implications for other

map recognition and automation control. However, it should be noted that this research method still has limitations in more precise motion control scenarios. Consequently, the proposed enhanced PTC algorithm is unable to handle path control tasks with low accuracy, such as subways and light rail.

3 Testing and analyzing the effect of V-MPC model application

The performance test of the V-MPC model is conducted on a desktop computer with i7-13700K CPU, GeForce RTX 3090 GAMER OC graphics card, and CentOS 7. The experiment utilizes the KITTI Vision Benchmark Suite (KITTI) and CARLA Simulator (CARLA) data sets, which contain sensor data from autonomous vehicles collected on real roads, including camera images and laser radar data. Although the KITTI and CARLA datasets provide a wealth of sensor and environmental data, there are some limitations to both datasets. KITTI data sets are mainly collected under clear weather conditions, which may limit their applicability in severe weather conditions such as rain and snow. Because CARLA is a simulation environment, its data may not fully simulate the complexity and variability of the real world. Therefore, to ensure control of experimental variables, all models participating in the performance analysis experiment will undergo a 2-hour pre-training session. The pre-training dataset will consist of randomly selected data samples from KITTI, while ensuring consistency between the pre-training system environment and hardware environment.

The control models used in this experiment are the particle swarm optimization-based PI controller model (PSO-PI) and the L6DOF. The double-shifted reference trajectories of the L6DOF model and the V-MPC model on the CARLA dataset are shown in Figure 6. Figure 6(a) represents the double-shifted line reference trajectory of the L6DOF model, from which it can be seen that the transverse position of the L6DOF model has a large magnitude of variation, indicating that the stability of the L6DOF model is poor. Figure 6(b) represents the double-shifted line reference trajectory of the V-MPC model, and the transverse position variation of the V-MPC model is smaller, indicating that the model is more stable.

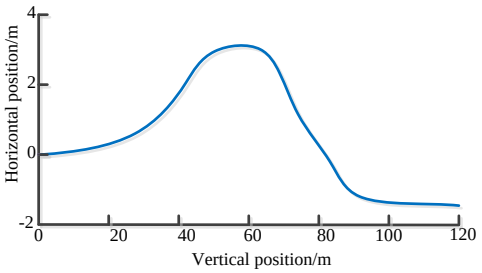

(a) L6DOF model double shift line reference trajectory

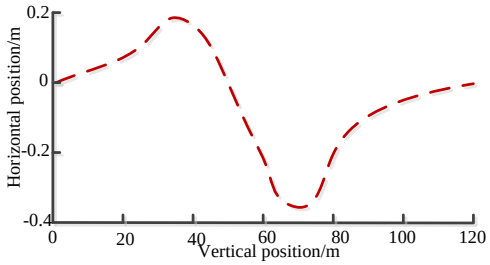

(b) V-MPC model double shift line reference trajectory

Figure 6: Reference trajectories of double moving lines for different models

Figure 7 compares the transverse errors of the V-MPC model and the L6DOF model at various speeds using the KITTI dataset. The lateral error findings of the

L6DOF model and the V-MPC model are shown in Figures 7(a) and 7(b), respectively. The error variation in the first half of the route is essentially the same for the two models, according to the data; nevertheless, the V-MPC model's error value is lower than the L6DOF models. Moreover, the error variation of V-MPC model in the second half of the journey is obviously better than the control model.

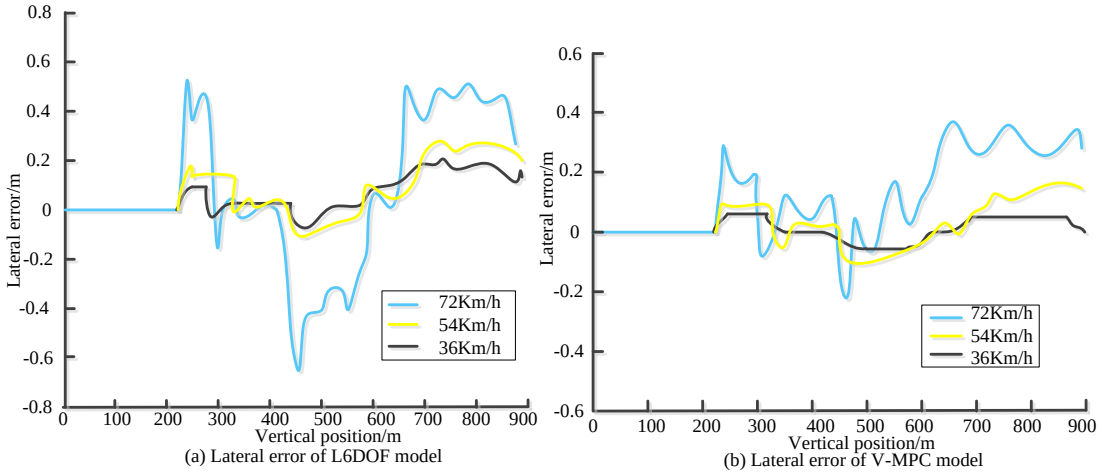

Figure 7: Comparison of lateral errors of different models

The comparison of path deviation prediction accuracy of PSO-PI model and V-MPC model is shown in Figure 8. The accuracy of each model's path deviation prediction using the CARLA dataset is shown in Figure 8(a). On this dataset, the V-MPC model's average accuracy is 88.33%, greater than the PSO-PI model's 84.64%. Figure 8(b) represents the path deviation prediction accuracy of different models on the KITTI dataset. Based on Figure 8(b), the V-MPC model has an average accuracy of 82.1%, which is 4.72% greater than the PSO-PI model.

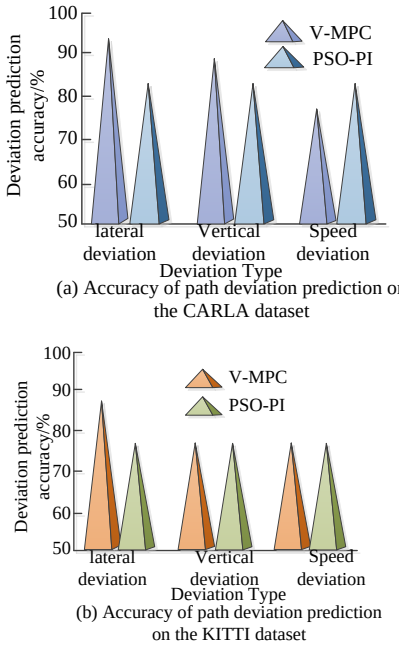

Figure 8: Comparison of accuracy of path deviation prediction among different models

The energy consumption metrics are employed to assess the optimized kinetic models' energy usage efficiency. Figure 9 shows a comparison of the PSO-PI and V-MPC models' energy consumption across various datasets. The energy usage of the models using the KITTI dataset is shown in Figure 9(a). The energy usage of the two models on the CARLA dataset is shown in Figure 9(b). In Figure 9, the change in energy consumption of V-MPC model with increasing distance traveled is smoother, so it is concluded that V-MPC model has better stability during operation.

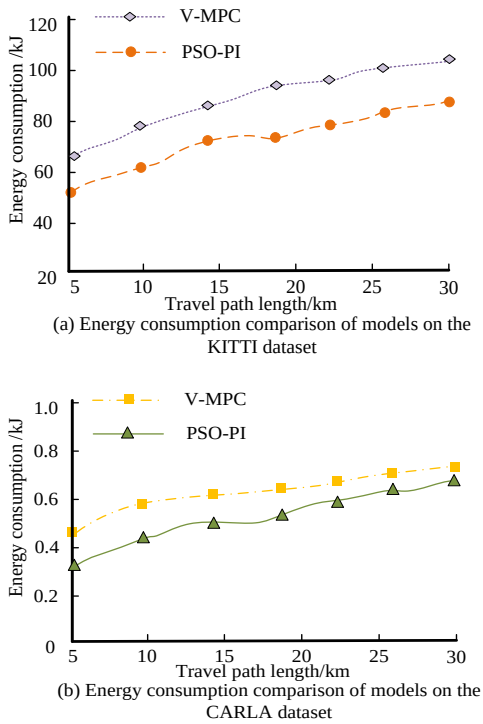

Figure 9: Comparison of energy consumption of different models

Figure 10 represents the variation of front wheel deflection angle and deflection increment versus time when the driverless car equipped with the V-MPC model is doing uniform circular motion. Figure 10(a) shows the

front wheel deflection angle versus time at different vehicle speeds, while Figure 10(b) shows the angular increment of front wheel deflection at different vehicle speeds. The sub-experiment tests the stability of the model steering by circular motion. In Figure 10, the curve fluctuation is minimized at a speed of 20km/h. Therefore, it is concluded that the steering stability of the vehicle segment is optimal when the initial speed is 20km/h in the experimental environment, while the speed is too fast or too slow will lead to the reduction of stability.

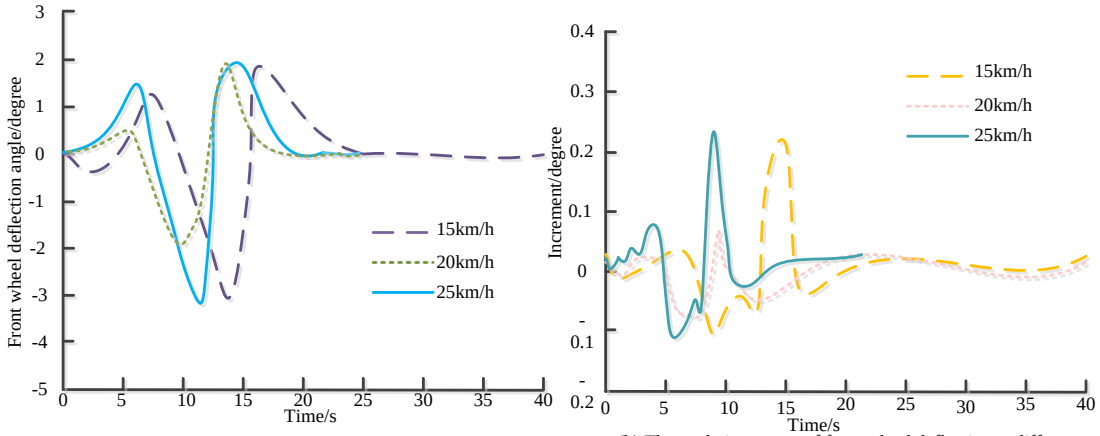

(a) The relationship between front wheel deflection angle and time at different vehicle speeds

(b) The angle increment of front wheel deflection at different vehicle speeds

Figure 10: Changes in the relationship between front wheel deflection angle and deflection increment with time

For the VSC algorithm, the controller switching frequency is an important index, and the controller switching frequency affects the response speed, stability and energy consumption. Figure 11 displays the findings of this study, which analyzes the controller switching frequencies of the three models—PSO-PI, V-MPC, and L6DOF—using various datasets. The controller switching frequencies of the three models on the KITTI and CARLA datasets are shown in Figures 11(a) and 11(b), respectively. The figures demonstrate that there is a considerable difference in switching frequency between the KITTI and CARLA datasets. It can also be concluded that the controller switching frequency decreases gradually when the speed is too large or too small, and peaks at a speed of 3-4 m/s.

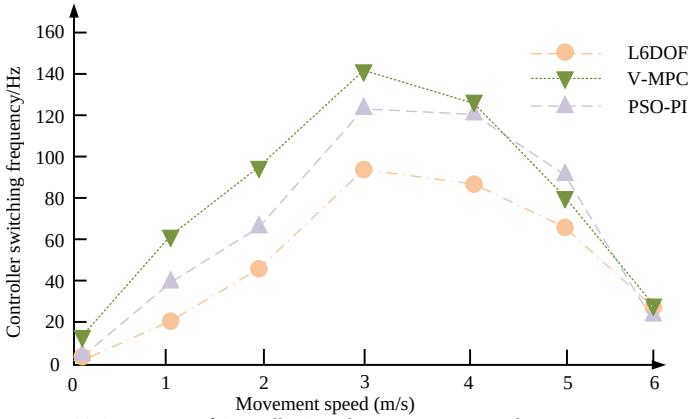

(a) Comparison of Controller Switching Frequencies on the KITTI Dataset

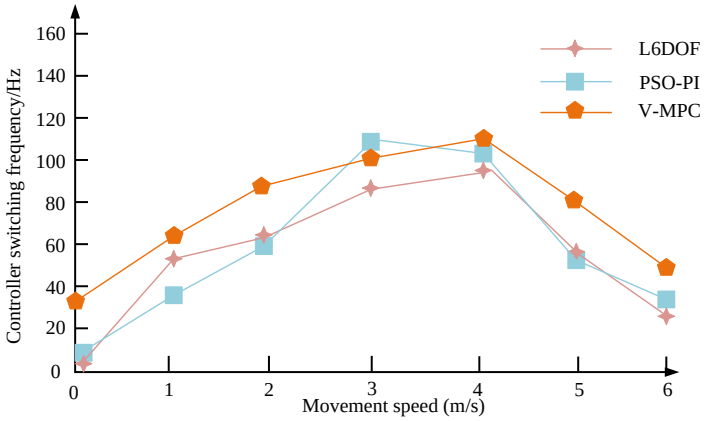

(b) Comparison of Controller Switching Frequencies on the CARLA Dataset

Figure 11: Comparison of switching frequencies of different model controllers

The control accuracy indicates the accuracy of the optimized dynamics model for the control inputs. Figure 12 displays a comparison of the three models' control accuracy using the KITTI and CARLA datasets: PSO-PI, V-MPC, and L6DOF. The control accuracy of the V-MPC model in Figure 12(a) is 94.19%, which is 8.73% higher than the L6DOF model and 4.70% higher than the PSO-PI model. Figure 12(a) shows the control accuracy of the three models on the KITTI dataset. Figure 12(b) represents the control accuracy of the three models on the CARLA dataset. Based on the experimental findings, the V-MPC model has a higher control precision with an accuracy of 95.61%, compared to the PSO-PI model with an accuracy of 91.76% and the L6DOF model with an accuracy of 81.62%.

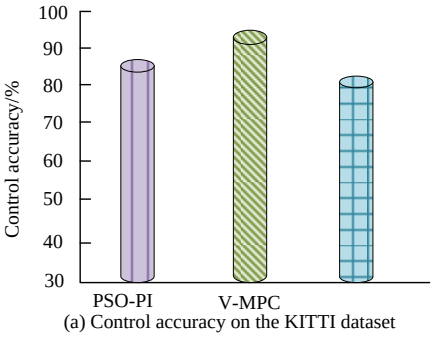

(a) Control accuracy on the KITTI dataset

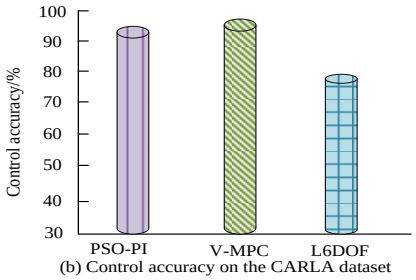

(b) Control accuracy on the CARLA dataset

Figure 12: Comparison of control accuracy of different models

To assess the complexity of the V-MPC, PSO-PI, and L6DOF algorithms, the KITTI and CARLA datasets are used as inputs, and the output time of the corresponding models can intuitively reflect the complexity of different algorithms. Figure 13 illustrates a comparison of the output times for each algorithm. Figure 13 (a) compares the complexity of the V-MPC, PSO-PI, and L6DOF models on the KITTI dataset, while Figure 13 (b) compares the complexity of different models on the CARLA dataset. The figures show that the V-MPC model has a shorter output time on both datasets (0.856s and 0.818s, respectively) compared to the PSO-PI and L6DOF models. Therefore, the proposed model is more progressive in terms of algorithm complexity. Based on the experiment results, it is evident that the proposed model has high control accuracy, making it suitable for scenarios with long driving times and high path accuracy requirements, such as unmanned express delivery. Additionally, the proposed model exhibits strong scalability. The MPC algorithm can introduce dynamic parameter optimization algorithms to accelerate the convergence speed and computational efficiency of the model because it predicts through a system dynamic model.

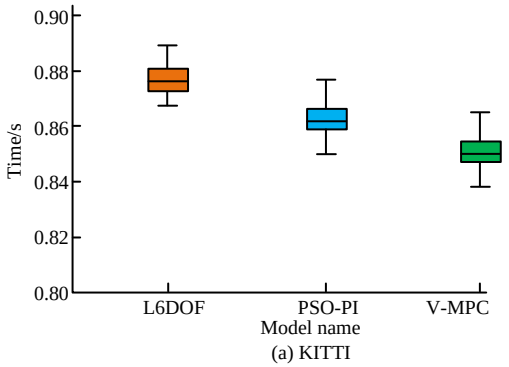

(a) KITTI

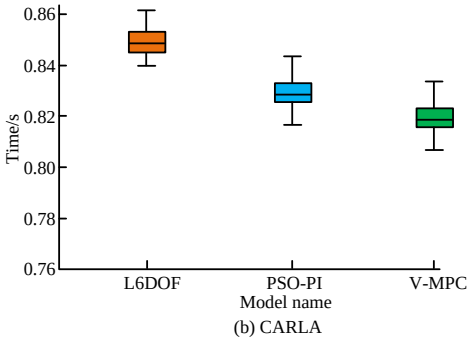

Figure 13: Schematic diagram of comparing the complexity of path tracking control using different algorithms

The study analyzes and compares errors generated by different models on the KITTI dataset. To eliminate accidental errors, the experiment is repeated three times. The results of the error comparison are presented in Figure 14, which shows that the V-MPC model has the lowest path judgment error rate among the three models. Additionally, the V-MPC model had an average error rate of 1.17% across all three experiments, while the PSO-PI model had an average error rate of 1.55%, and the L6DOF model had an average error rate of 1.69%. Based on the error analysis results, it can be concluded that the proposed model has minimal errors and is suitable for high-accuracy automated path selection scenarios.

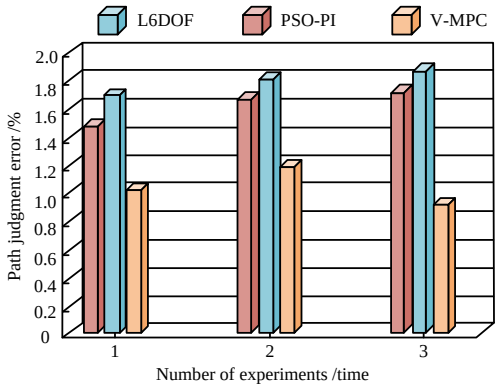

Figure 14: Comparison diagram of error analysis for different models

Based on the experiment results, it is evident that the proposed model has high control accuracy and energy utilization efficiency, making it suitable for scenarios with long driving times and high path accuracy requirements, such as unmanned express delivery. Additionally, the proposed model exhibits strong scalability. The MPC algorithm can introduce dynamic parameter optimization algorithms to accelerate the convergence speed and computational efficiency of the model because it predicts through a system dynamic model.

4 Discussion

In recent years, with the rapid development of the logistics industry, there has been a great deal of interest in free vehicles due to their high efficiency and intelligence. Firstly, in terms of PTC, existing research has predominantly employed algorithms based on deep neural networks and sliding mode control, which have yielded satisfactory tracking outcomes, such as the deep neural network optimization control system proposed by Chen et al [7]. and the fast nonsingular terminal sliding mode control strategy proposed by Sun et al [9]. Secondly, previous studies have demonstrated the efficacy of MPC as a control strategy. This included the multi-layer graph architecture based on MPC proposed by Pan et al [10]. and the load/frequency controller based on MPC proposed by Beus et al [12]. By optimizing the objective function and constraint conditions of the MPC algorithm, the control system can operate in an efficient manner. Finally, existing research has demonstrated the advantages of the ULV algorithm in improving vehicle roll stability and control smoothness. For instance, the integrated control method combining MPC and ULV algorithm proposed by Lin et al [8] has been shown to be effective. However, current research still faces challenges in terms of computational complexity and implementation. Consequently, the research combines the VSC and MPC algorithms and optimizes the 6-degree-of-freedom vehicle dynamics model in order to overcome the shortcomings of existing research and achieve more stable and efficient ULV control. The optimized model has improved significantly in terms of computational complexity, output time, and control accuracy. This is due to the VSC algorithm simplifying the model's structure, which avoids unnecessary calculations. Additionally, the MPC algorithm optimizes the objective and output functions of the model, allowing for accurate analysis and path selection. After introducing the VSC and MPC algorithms, the performance of the linear six-degree-of-freedom vehicle dynamics model has significantly improved. This model can be applied to industries such as unmanned logistics and unmanned food delivery due to its fast output capability, which enhances its adaptability and expands its application space.

5 Conclusion

This research delves into ULV control based on ULV algorithms. High-precision navigation and control of ULVs is achieved through advanced ULV algorithms and dynamics modeling techniques. The technique not only offers a fresh approach to ULV control, but it also establishes the framework for the automated and intelligent creation of next-generation logistics systems. The experimental findings showed that on two distinct datasets, the suggested model performed better than the control model. In terms of path deviation prediction, the average accuracy of the proposed model on the two

datasets was 88.33% and 82.1%, which was 3.96% and 4.72% better than the control model, respectively. This result proved the advantage of the proposed model in terms of prediction accuracy. Also the control accuracy of the proposed model reached 94.19% on the KITTI dataset and 95.61% on the CARLA dataset, both of which are higher than other control models. In addition to the above two metrics, the study also tested other aspects of the model, including energy consumption, controller switching frequency and lateral error. The experimental results verify that the suggested model exhibits a decent level of sophistication and performs comparably across various criteria.

Furthermore, in consideration of the complex and unpredictable nature of real-world logistics scenarios, the study employed a substantial number of data samples to train Jupiter, ensuring that the training data samples encompass the majority of potential scenarios in real-world logistics. Concurrently, in actual unmanned logistics workshops, the range of activities performed by different transfer vehicles is relatively limited. Consequently, the study employs path tracking algorithms to ensure that the model possesses the requisite dynamic and unpredictable capabilities to cope with real-world scenarios following autonomous selection.

6 Ethical and safety considerations

The use of UAVs or drones in modern logistics is becoming increasingly prevalent. As such, it is of paramount importance to ensure that their use is safe and ethical. Research in this field adheres to the highest ethical standards in order to minimize the potential risks that UAVs may face in their autonomous decision-making process. Throughout the entire development process of UAVs, relevant safety protocols have been developed to prevent potential accidents. At the same time, a protection mechanism is set up in UAVs, which can switch to manual control in case of system failure, ensuring safety during transportation. Finally, the study will implement rigorous privacy protection measures in accordance with global data security standards.

Acknowledgement

The research is supported by 2023 Henan University Humanities and Social Sciences Research General Project, Research on the innovative development of urban green logistics distribution under the "Carbon peaking and Carbon neutrality" goals, 2023-ZDJH-108.

References

[1] Z. Sun, Q. Wang, L. Chen, and C. Hu, "Unmanned technology-based civil-military intelligent logistics system: from construction to integration," Journal of Beijing Institute of Technology, vol. 31, no. 2, pp. 140-151, 2022. https://doi.org/10.15918/j.jbit1004-0579.2022.010

[2] A. Kamat, S. Shanker, and A. Barve, "Assessing the factors affecting implementation of unmanned aerial vehicles in Indian humanitarian logistics: a g-DANP approach," Journal of Modelling in Management, vol. 18, no. 2, pp. 416-456, 2023. https://doi.org/10.1108/jm2-02-2021-0037

[3] J. Gu, "Risk prediction of enterprise credit financing using machine learning," Informatica, vol. 46, no. 7, pp. 145, 2022. https://doi.org/10.31449/inf.v46i7.4247

[4] K. L. Choi, M. J. Kim, and Y. M. Kim, "On safety improvement through process establishment for SOTIF application of autonomous driving logistics robot," International Journal of Internet, Broadcasting and Communication, vol. 14, no. 1, pp. 209-218, 2022. https://doi.org/10.7236/IJIBC.2022.14.1.209

[5] G. Iannace, G. Ciaburro, and A. Trematerra, "Acoustical unmanned aerial vehicle detection in indoor scenarios using logistic regression model," Building Acoustics, vol. 28, no. 1, pp. 77-96, 2021. https://doi.org/10.1177/1351010X20917856

[6] P. Hang, and X. Chen, "Path tracking control of 4-wheel-steering autonomous ground vehicles based on linear parameter-varying system with experimental verification," Proceedings of the Institution of Mechanical Engineers, Part I: Journal of Systems and Control Engineering, vol. 235, no. 3, pp. 411-423, 2021. https://doi.org/10.1177/0959651820934572

[7] I. M. Chen, and C. Y. Chan, "Deep reinforcement learning based path tracking controller for autonomous vehicle," Proceedings of the Institution of Mechanical Engineers, Part D: Journal of Automobile Engineering, vol. 235, no. 2-3, pp. 541-551, 2021. https://doi.org/10.1177/0954407020954591

[8] F. Lin, S. Wang, Y. Zhao, and Y. Cai, "Research on autonomous vehicle path tracking control considering roll stability," Proceedings of the Institution of Mechanical Engineers, Part D: Journal of Automobile Engineering, vol. 235, no. 1, pp. 199-210, 2021. https://doi.org/10.1177/0954407020942006

[9] Z. Sun, J. Zou, D. He, and W. Zhu, "Path-tracking control for autonomous vehicles using double-hidden-layer output feedback neural network fast nonsingular terminal sliding mode," Neural Computing and Applications, vol. 34, no. 7, pp. 5135-5150, 2022. https://doi.org/10.1007/s00521-021-06101-8

[10] Z. Pan, Z. Sun, H. Deng, and D. Li, "A multilayer graph for multiagent formation and trajectory tracking control based on MPC algorithm," IEEE Transactions on Cybernetics, vol. 52, no. 12, pp.

13586-13597, 2021. https://doi.org/10.1109/TCYB.2021.3119330

[11] M. E. Çimen, and Y. Yalçın, "A novel hybrid firefly–whale optimization algorithm and its application to optimization of MPC parameters," Soft Computing, vol. 26, no. 4, pp. 1845-1872, 2022. https://doi.org/10.1007/s00500-021-06441-6

[12] M. Beus, and H. Pandžić, "Practical implementation of a hydro power unit active power regulation based on an mpc algorithm," IEEE Transactions on Energy Conversion, vol. 37, no. 1, pp. 243-253, 2021. https://doi.org/10.1109/TEC.2021.3094059

[13] W. J. Liu, H. F. Ding, M. F. Ge, and X. Y. Yao, "Cooperative control for platoon generation of vehicle-to-vehicle networks: a hierarchical nonlinear MPC algorithm," Nonlinear Dynamics, vol. 108, no. 4, pp. 3561-3578, 2022. https://doi.org/10.1007/s11071-022-07400-y

[14] G. Veselov, A. Tselykh, A. Sharma, and R. H. Huang, "Applications of artificial intelligence in evolution of smart cities and societies," Informatica, vol. 45, no. 5, 2021. https://doi.org/10.31449/inf.v45i5.3600

[15] H. Wang, T. Zhang, X. Zhang, and Q. Li, "Observer-based path tracking controller design for autonomous ground vehicles with input saturation," IEEE/CAA Journal of Automatica Sinica, vol. 10, no. 3, pp. 749-761, 2023. https://doi.org/10.1109/JAS.2023.123078

[16] N. Wang, Y. Zhang, C. K. Ahn, and Q. Xu, "Autonomous pilot of unmanned surface vehicles: Bridging path planning and tracking," IEEE Transactions on Vehicular Technology, vol. 71, no. 3, pp. 2358-2374, 2021. https://doi.org/10.1109/TVT.2021.3136670

[17] S. Feng, Y. Qian, and Y. Wang, "Collision avoidance method of autonomous vehicle based on improved artificial potential field algorithm," Proceedings of the Institution of Mechanical Engineers, Part D: Journal of Automobile Engineering, vol. 235, no. 14, pp. 3416-3430, 2021. https://doi.org/10.1177/09544070211014319

[18] M. Labbadi, and M. Cherkaoui, "Adaptive fractional-order nonsingular fast terminal sliding mode based robust tracking control of quadrotor UAV with Gaussian random disturbances and uncertainties," IEEE Transactions on Aerospace and Electronic Systems, vol. 57, no. 4, pp. 2265-2277, 2021. https://doi.org/10.1109/TAES.2021.3053109

[19] S. Wallace, and G. Lăzăroiu, "Predictive control algorithms, real-world connected vehicle data, and smart mobility technologies in intelligent transportation planning and engineering," Contemporary Readings in Law and Social Justice, vol. 13, no. 2, pp. 79-92, 2021. https://doi.org/10.22381/CRLSJ13220216

[20] A. Williams, "Human-centric functional computing as an approach to human-like computation," Artificial Intelligence and Applications, vol. 1, no. 2, pp. 118-137, 2023. https://doi.org/10.47852/bonviewAIA2202331

[21] G. Bandewad, K. P. Datta, B. W. Gawali, and S. N. Pawar, "Review on discrimination of hazardous gases by smart sensing technology," Artificial Intelligence and Applications, vol. 1, no. 2, pp. 86-97, 2023. https://doi.org/10.47852/bonviewAIA3202434

[22] J. Jin, and J. Gong, "An interference-tolerant fast convergence zeroing neural network for dynamic matrix inversion and its application to mobile manipulator path tracking," Alexandria Engineering Journal, vol. 60, no. 1, pp. 659-669, 2021. https://doi.org/10.1016/j.aej.2020.09.059

[23] P. M. Marusak, "A numerically efficient fuzzy MPC algorithm with fast generation of the control signal," International Journal of Applied Mathematics and Computer Science, vol. 31, no. 1, pp. 59-71, 2021. https://doi.org/10.34768/amcs-2021-0005

[24] D. Wang, Q. Chen, X. Zhang, C. Gao, B. Wang, X. Huang, and J. Crittenden, "Multipollutant control (MPC) of flue gas from stationary sources using SCR technology: A critical review," Environmental Science & Technology, vol. 55, no. 5, pp. 2743-2766, 2021. https://doi.org/10.1021/acs.est.0c07326